The cryosphere

Supplementary Materials for

A process-based perspective on Antarctic sea ice regimes using objective data mining

Jinfei Wang[1,2], Maike Sonnewald[3,4,5], Noé Pirlet[2], François Massonnet[2], Hugues Goosse[2], Dake Chen[1], Qinghua Yang[1]

[1]School of Atmospheric Sciences, Sun Yat-sen University, and Southern Marine Science and Engineering Guangdong Laboratory (Zhuhai), Zhuhai, 519082, China
[2]Earth and Climate Center, Earth and Life Institute, Université catholique de Louvain, Louvain-la-Neuve, 1348, Belgium
[3]Department of Computer Science, University of California, Davis, 95616, USA
[4]University of Washington, Seattle, 98195, USA
[5]NOAA/Geophysical Fluid Dynamics Laboratory, Princeton, 08540, USA

Correspondence to: Qinghua Yang (yangqh25@mail.sysu.edu.cn)

This PDF file includes:

Figures. S1 to S11
Table S1

Other Supplementary Materials for this manuscript include the following:

Movie S1

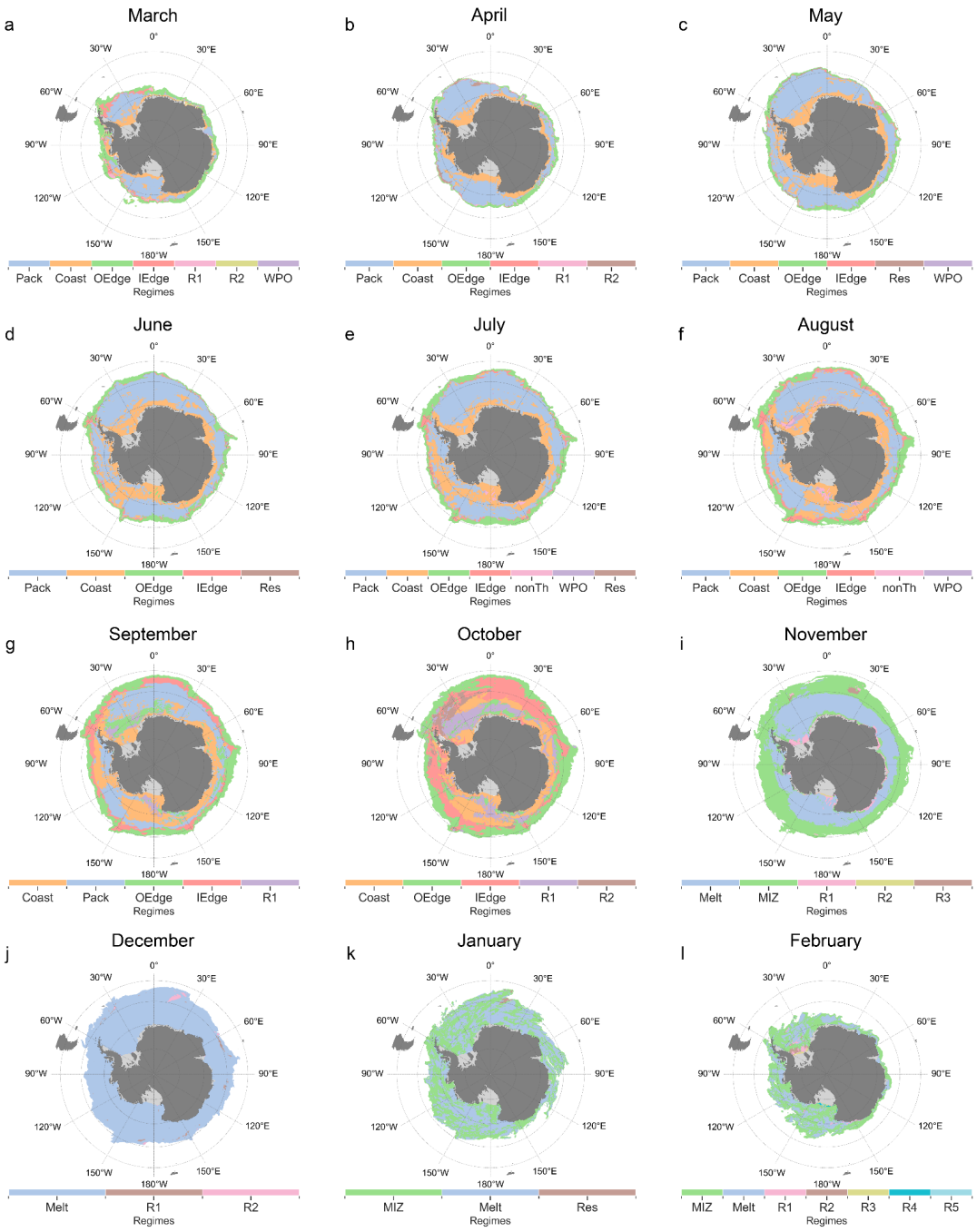

Figure S1. Monthly clustering results displayed on geographical maps. The clustering was performed using the same methodology as for the growth season (March–September). Regimes are named based on their dominant dynamic and thermodynamic characteristics (see Figure S2), following the classification used for the growth season. Less distinct or noisy regimes are labeled as R1–R5.

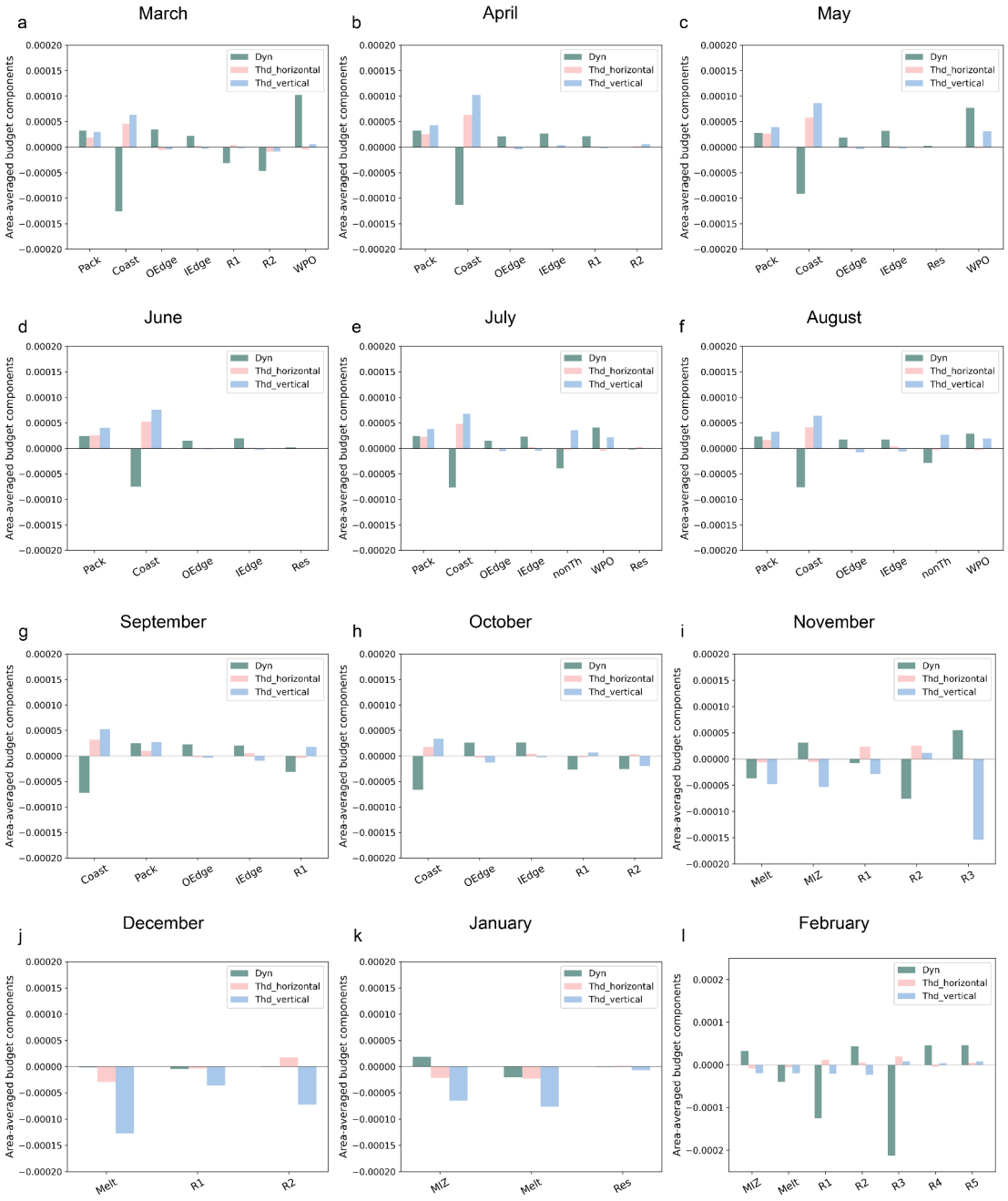

Figure S2. Area-averaged budget components (Unit: kg m^{-2} s^{-1}) for each individual month.

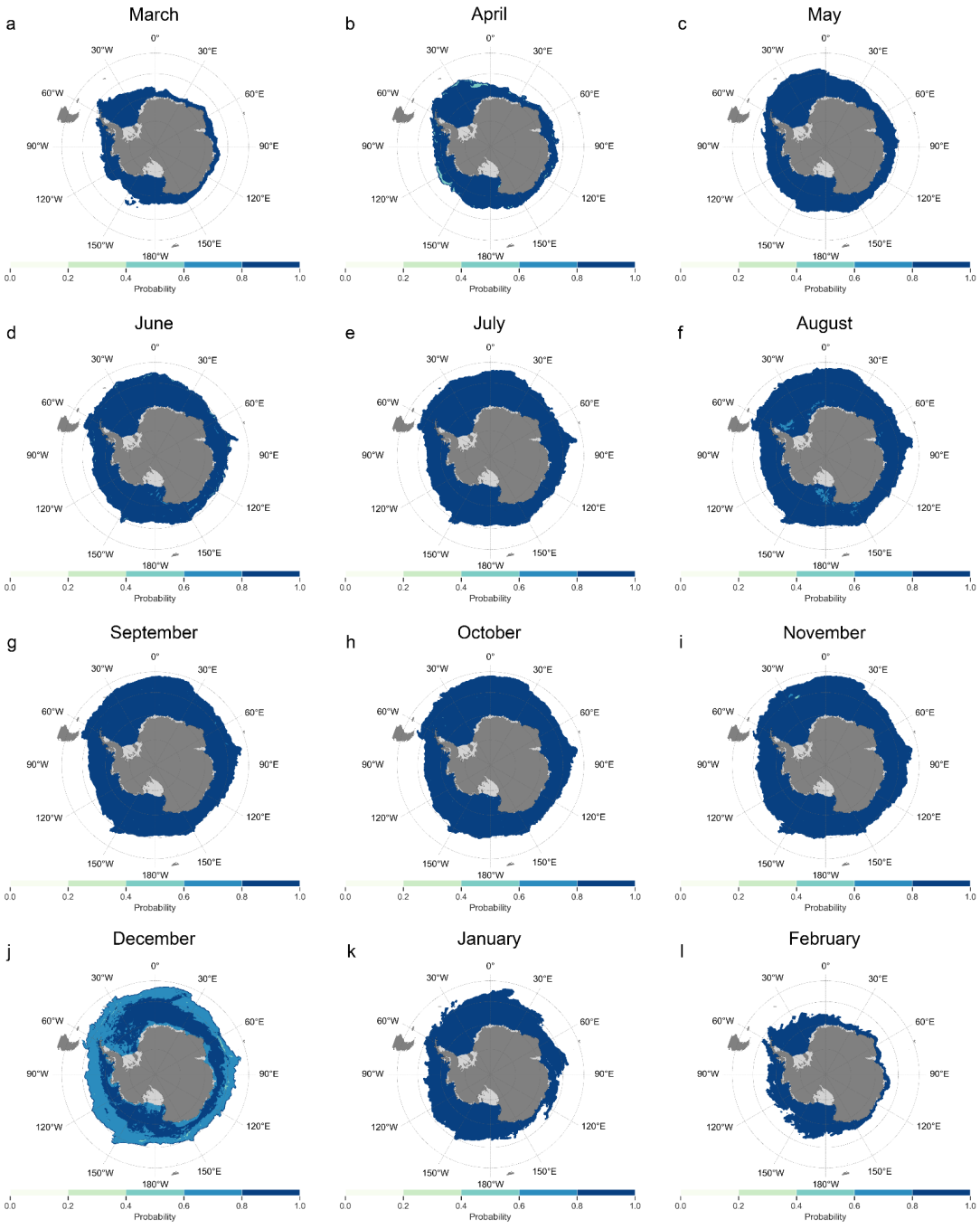

Figure S3. Probability of occurrence for each final cluster across 100 iterations for individual months, illustrating the robustness of the clustering results.

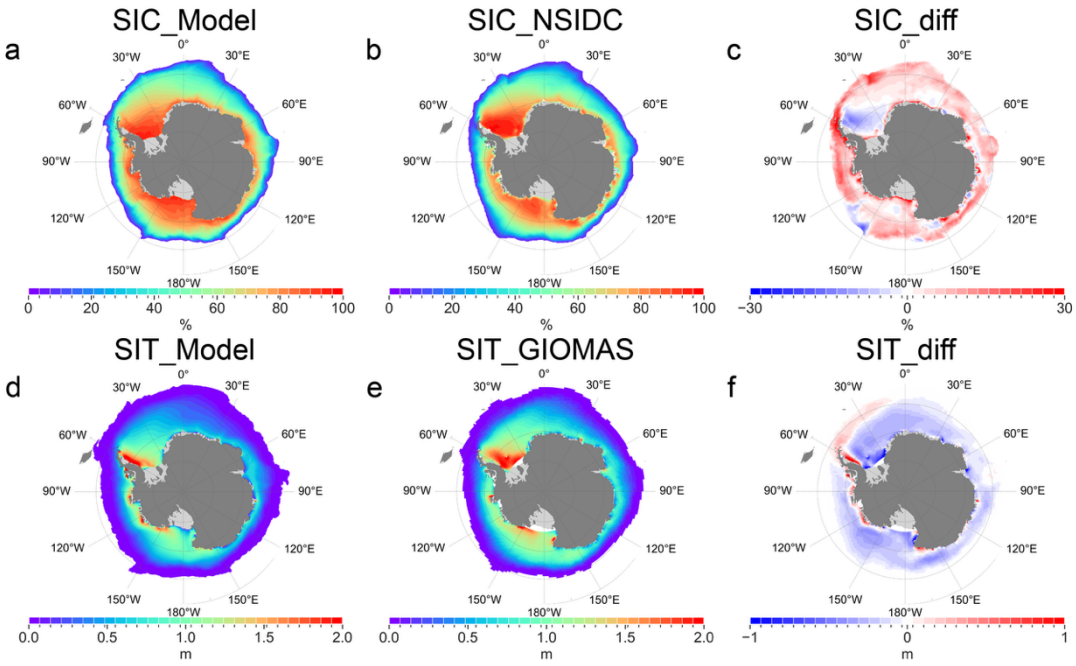

Figure S4. (a) Modeled climatological Sea Ice Concentration (SIC) during the growth season (March–September) averaged over 1981–2010. (b) Observed SIC from the National Snow and Ice Data Center (NSIDC) for the same period. (c) Difference between the modeled and observed SIC. (d) Modeled climatological Sea Ice Thickness (SIT) during the growth season (March–September) averaged over 1981–2010. (e) SIT reanalysis from the Global Ice–Ocean Modeling and Assimilation System (GIOMAS) for the same period. (f) Difference between the modeled and reanalysis SIT.

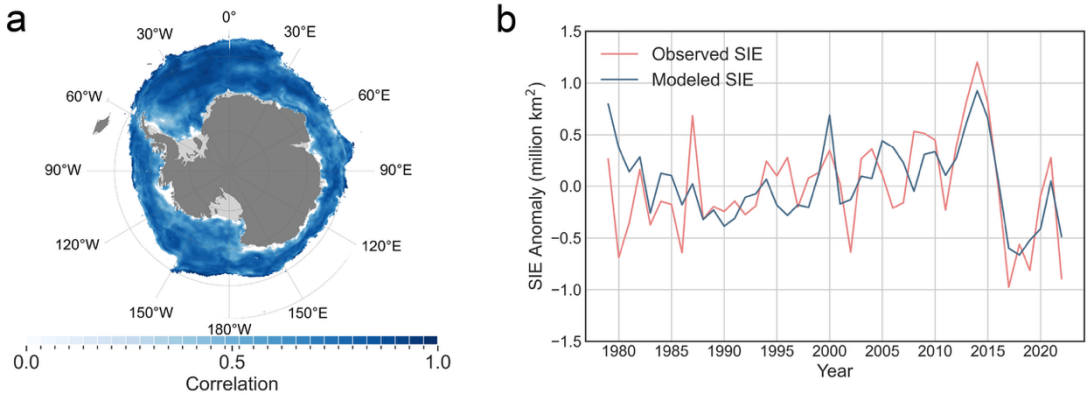

Figure S5. (a) Spatial correlation map between observed SIC from NSIDC and modeled SIC, averaged over the growth season (March–September) during 1979–2023. Only areas that pass the 95% significance test are displayed. (b) SIE time series of observed SIC from NSIDC and modeled SIC, averaged over the growth season (March–September) during 1979–2023.

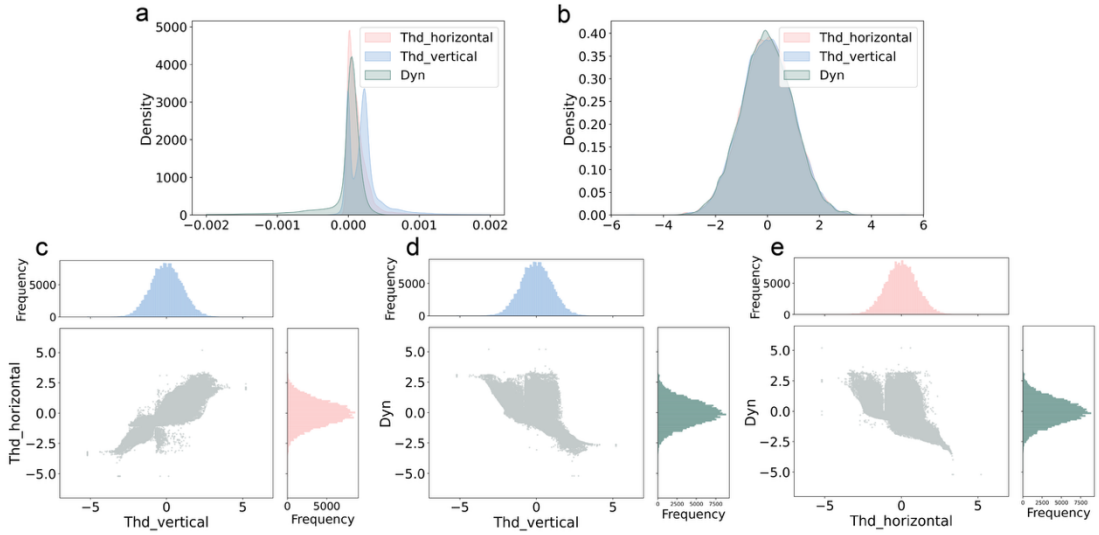

Figure S6. (a) Kernel density estimations (KDE) for the vertical thermodynamics, horizontal thermodynamics and dynamics before scaling with quantile transformer. (b) Same as (a) but after scaling with a quantile transformer. (c-e) Relationships among scaled vertical thermodynamics, horizontal thermodynamics and dynamics and the corresponding density distributions.

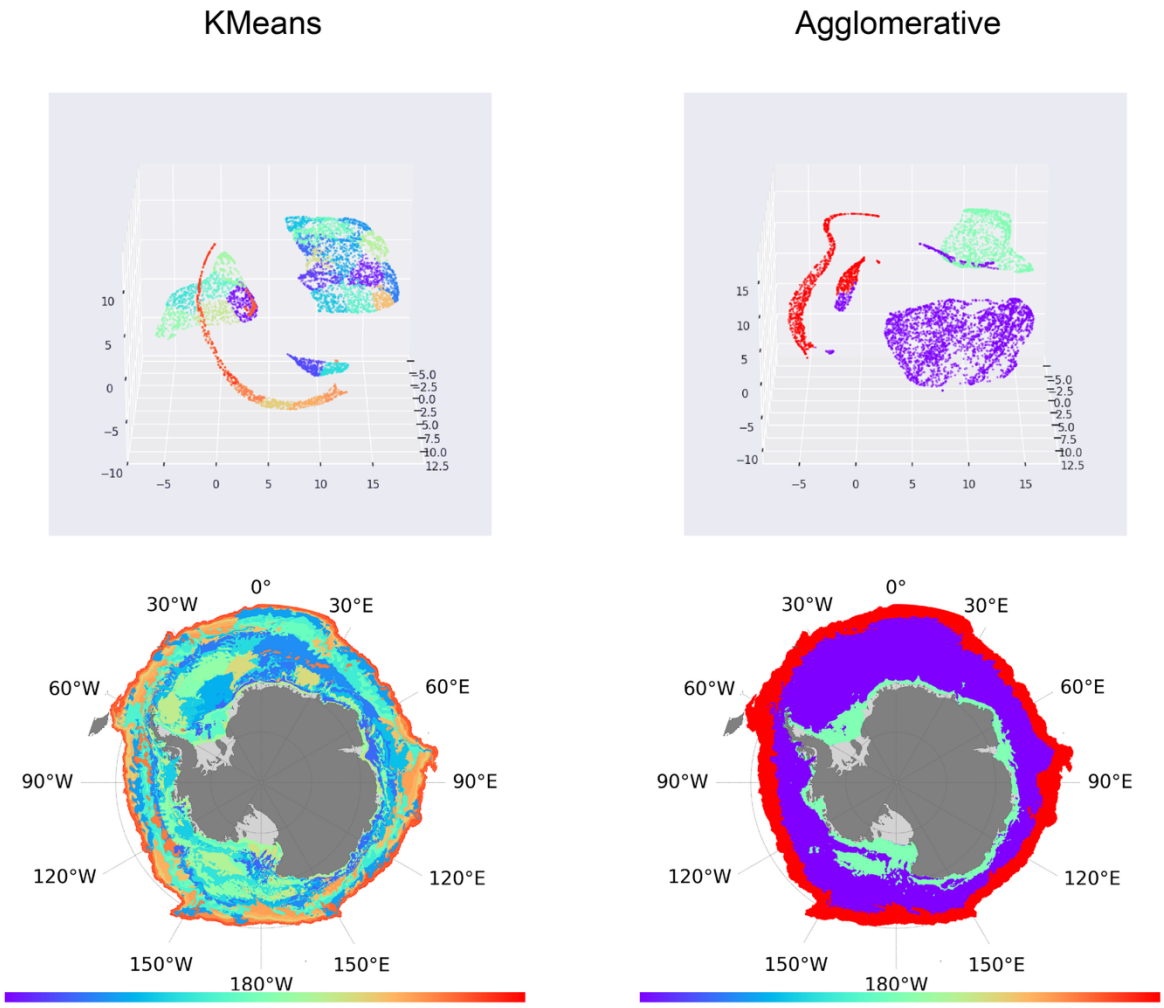

Figure S7: Comparison of results from KMeans clustering and Agglomerative clustering based on the same embedding process.

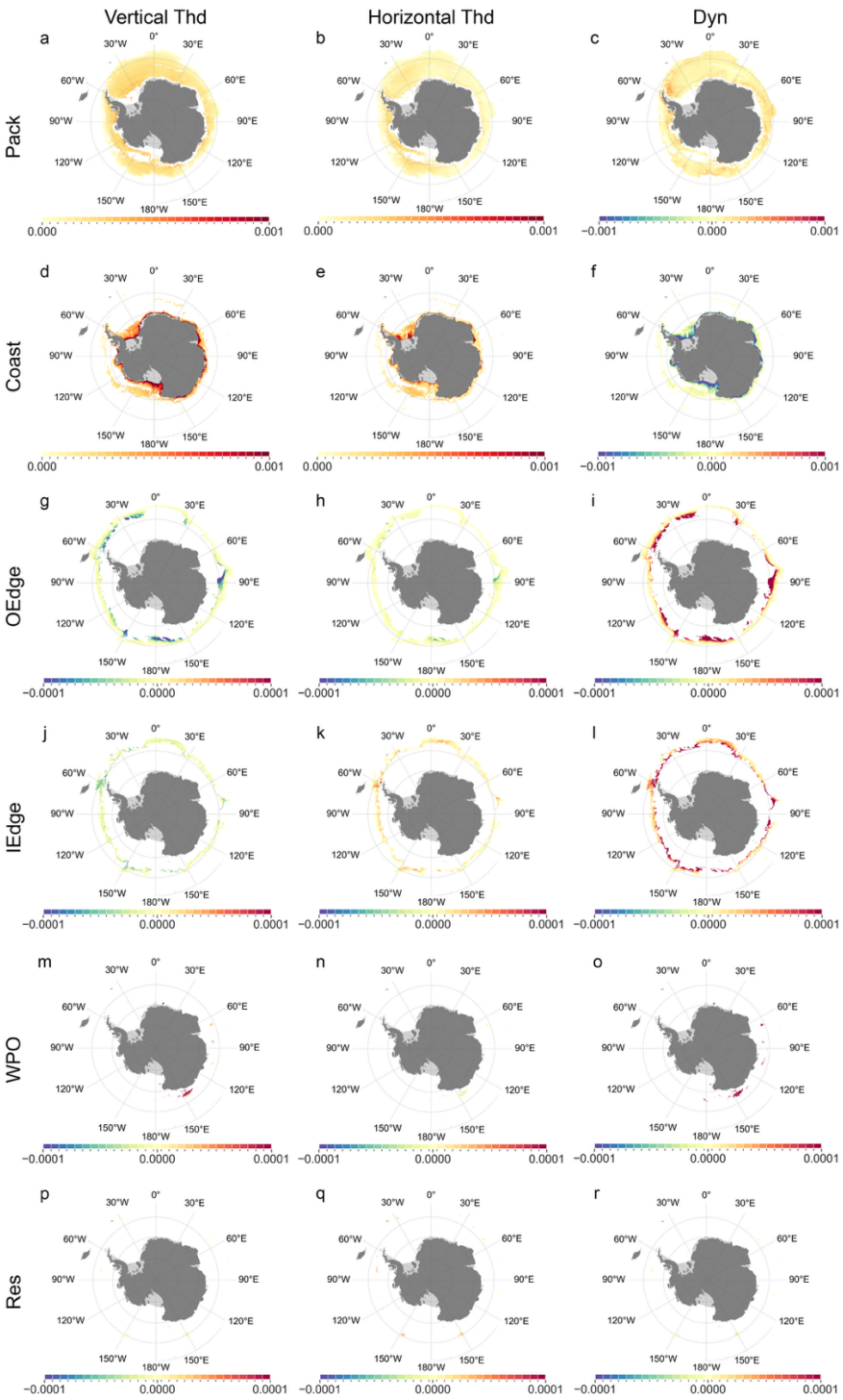

Figure S8. The spatial distributions of the budget terms in each cluster (Unit: kg m^{-2} s^{-1}). (a–c) represents vertical thermodynamic, horizontal thermodynamic and dynamic terms in the 'Pack' regime; (d-f) 'Coast' regime; (g-i) 'OEdge' regime; (j-l) 'IEdge' regime; (m-o) 'WPO' regime; (p-r) 'Res' regime. Note that different ranges of color bars are used to better emphasize the smaller values.

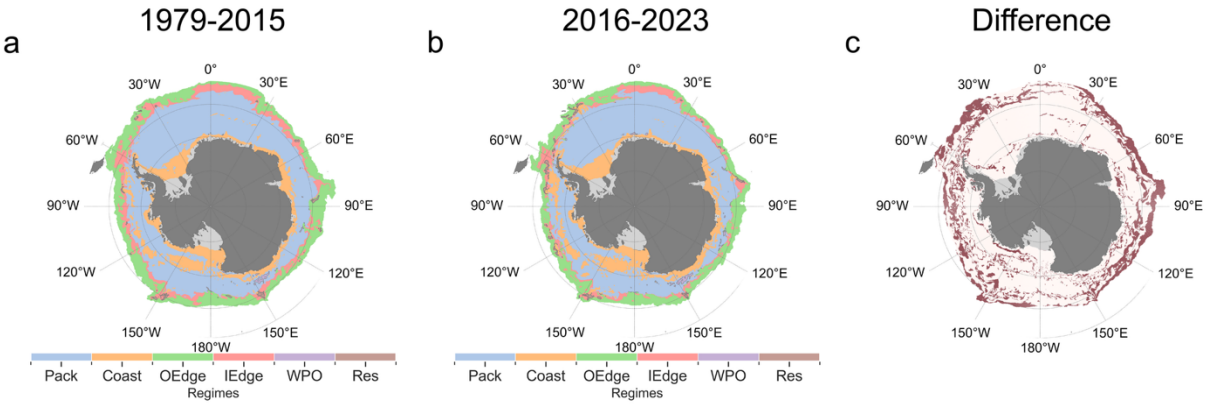

Figure S9. (a) Sea ice regime obtained from average sea ice budget components during 1979–2015. (b) Same as (a) but for 2016–2023. (c) Map of grid cells that changed regime between the two periods (from 1979–2015 to 2016–2023).

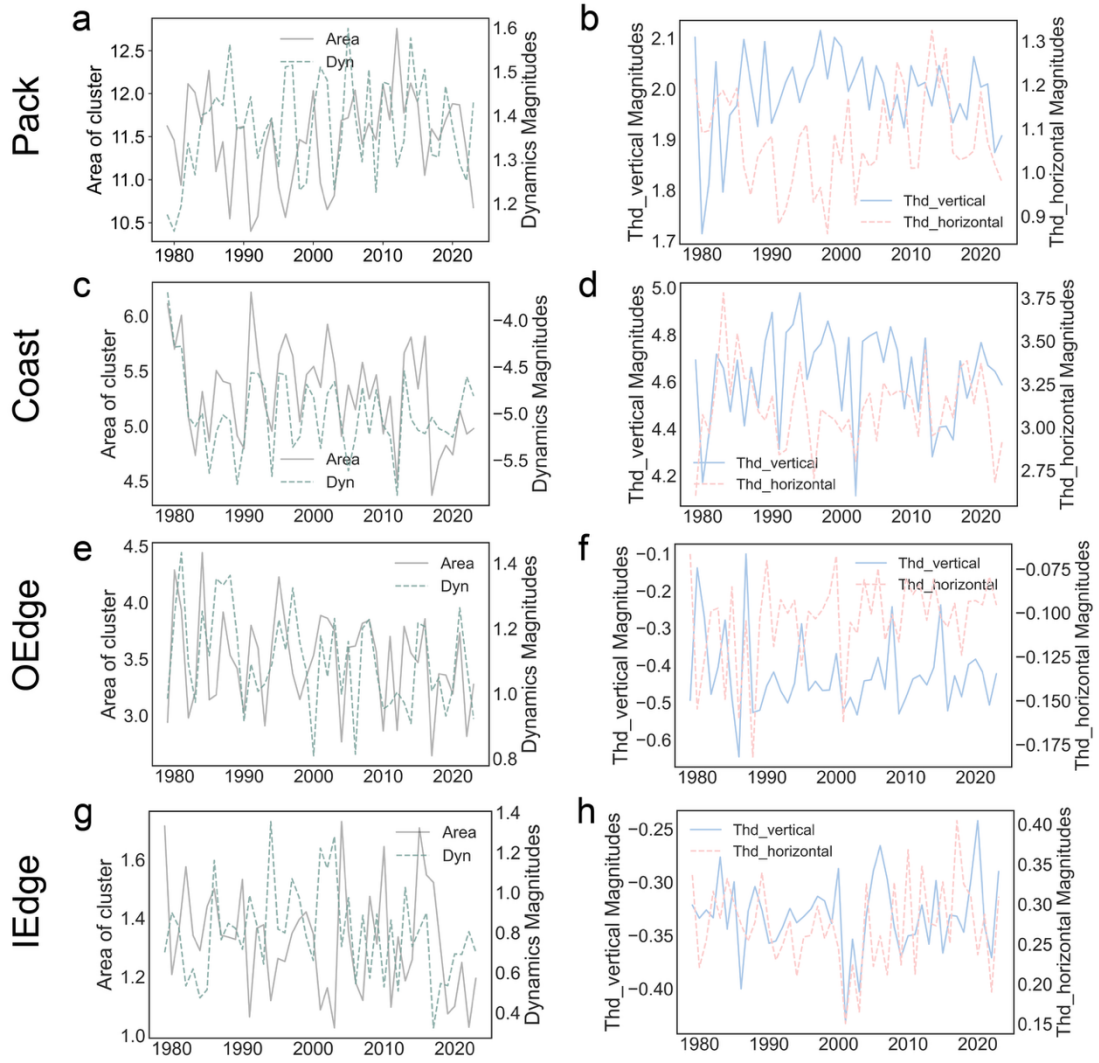

Figure S10. (a, c, e, g) Time series of regime area (Unit: million km^2) and dynamic magnitudes (Unit: 10^{-4} kg m^{-2} s^{-1}) for 'Pack', 'Coast', 'OEdge', 'IEdge' from 1979 to 2023. (b, d, f, h) Time series of vertical and horizontal thermodynamic magnitudes (Unit: 10^{-4} kg m^{-2} s^{-1}) for 'Pack', 'Coast', 'OEdge', 'IEdge' from 1979 to 2023. Analyses for additional clusters are not shown due to intermittent absence of additional clusters in certain years.

Regime	Trend_dyn (1979–2015)	Trend_dyn (2016–2023)	Trend_thd_v (1979–2015)	Trend_thd_v (2016–2023)	Trend_thd_h (1979–2015)	Trend_thd_h (2016–2023)
Pack	0.04	-0.11	0.02	-0.06	0.02	-0.03
Coast	-0.11	**0.66**	0.00	0.24	-0.01	-0.58
OEdge	**-0.05**	-0.10	-0.01	0.06	0.01	0.03
IEdge	0.02	0.19	0.00	0.02	0.00	-0.10

Table S1. Trends (kg m^{-2} s^{-1} $decade^{-1}$) of dynamic and thermodynamic components for 1979–2015 and 2016–2023. Bold indicates significance at 95% confidence.

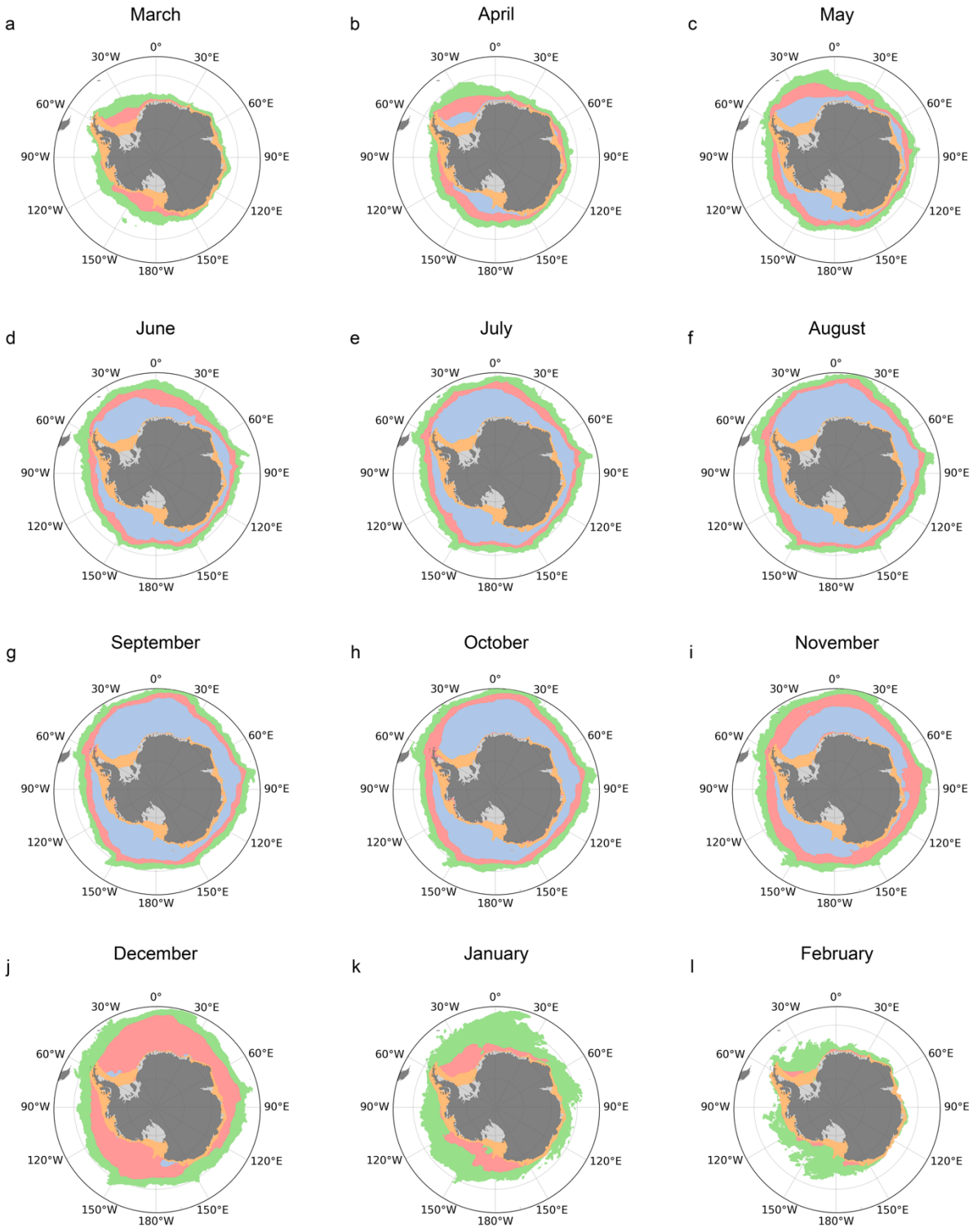

Figure S11. Climatological monthly sea ice classifications for 1981–2010 based on simple threshold criteria: low SIC (0–15%) in green, marginal ice zone (15–80%) in red, pack ice (80–100%) in blue, and coastal ice within 1000 m bathymetry in yellow.